

NSF GRANT # DMI - 0500453

NSF PRORAM NAME: Materials Processing & Manufacturing

## **GOALI:**

### **Online Dynamic Control of Cooling in Continuous Casting of Thin Steel Slabs**

**B.G. Thomas (PI)**

University of Illinois at Urbana-Champaign  
Department of Mechanical Science and Engineering  
1206 West Green Street, Urbana, IL 61801  
Email: bgthomas@uiuc.edu

**J. Bentsman (co-PI), B. Petrus, S. Vapalahti, H. Li**

University of Illinois, Urbana, Illinois

**A.H. Castillejos and F.A. Acosta**

Cinvestav, Saltillo, Mexico

**Abstract:** An online control system is being developed of secondary cooling for continuous casting machines in commercial steel plants, in order to maintain desired temperature setpoints in real time. This is important to optimize the quality of continuous-cast semi-finished steel shapes, which are used for 96% of the 100 million tons of steel produced in the U.S. each year.

The system features a fast, accurate transient computer model of heat transfer during the solidification process that serves as a “software sensor”, to provide feedback to a control system. Operating conditions are input from the level 2 automation system and the spray-water flow rates in the secondary cooling zone of the caster are continuously adjusted, in order to maintain the desired temperature profile throughout the steel. The system is being calibrated, using thermocouple and optical temperature sensors, tested and implemented at an operating U.S. thin slab caster.

In the second year of this large project, progress has been on several different subprojects. The transient finite difference model, CONID, has been optimized to run in an online environment and serves as the software sensor. A new control system has been developed using CONID and has been demonstrated to be capable of

stable tracking of the setpoints in real time, using a robust control algorithm that features anti-windup. Testing has shown it outperforms the existing control system used at the steel plant. It is currently being subjected to further rigorous testing under plant conditions. An ambitious experimental program to measure spray cooling coefficients has begun, including a novel induction-heating system that is capable of measuring heat transfer rates at constant surface temperature. Pyrometer measurements have been made at the steel plant to validate the temperature predictions. Finally, related work is proceeding on controlling fluid flow in the mold and in understanding of defect formation, in order to facilitate setpoint generation, so that cracks and other defects can be minimized.

Future improvements to this novel model-based control system could revolutionize the control of continuous casting spray systems, with improved steel quality, and will have beneficial impact on related scientific fields and commercial processes.

**1. Introduction:** For the high-volume low-profit-margin steel industry to compete in the world market, it must improve efficiency and consistency of steel quality. Implementing better control systems for the

continuous casting process is one way to achieve this. Continuous casting produces 96% of steel in the U.S. and the fraction of the new high-speed thin-slab casting process is growing every year<sup>[1]</sup>. Temperature variations during cooling in this process cause quality problems such as cracks, especially under transient conditions. Due to the high casting speeds and short response times, setting the spray water flow rates to maintain optimal temperature profiles during process changes becomes for operators increasingly difficult. Conventional feedback control systems cannot, however, be used for this purpose due to the insufficient reliability of temperature sensors. Recent model-based predictive control systems face special problems in thin slab casting, owing to the higher speed and the increased relative importance of solidification in the mold, which is not easy to predict accurately.

Previous studies, including those of the principal investigators, have developed comprehensive and efficient computational models of the continuous casting process based on nonlinear parabolic partial differential equations (PDEs). The accuracy of these models to predict heat transfer and solidification has been demonstrated through comparison with analytical solutions and plant measurements. This work has led to improved fundamental insights into the process. The next steps, proposed in this work, are 1) to more tightly tune these models to the thin slab casting and 2) to implement the knowledge contained in these models into a fundamentally-based system to dynamically control the water flow rates for cooling optimization. Since the thin slab casting process is in general characterized by nonlinear, spatially distributed, often time-varying, and relatively fast dynamics, a highly nontrivial control research and implementation effort is required to ensure robust optimal performance of spray cooling control systems.

Thus, the intellectual merit of this research is in i) providing a model of thin slab continuous casting using based on one-time plant measurements obtained at the caster specifically instrumented for this purpose, ii) developing novel state estimation and control design tools, applicable to systems governed by a class of nonlinear parabolic PDEs of interest, and iii) through the application of the tools developed to the refined thin slab continuous casting model, addressing implementation issues by synthesizing the first online temperature profile “software sensor” calibrated in real time through reliable online measurements, and deriving the optimal spray cooling control algorithms using this sensor.

This effort combines the talents of a team of researchers, including the experience of B.G. Thomas in mathematical modeling of continuous casting, Prof. J.

Bentsman in adaptive control theory of distributed parameter systems and predictive control, experienced student researchers to carry out the work, and an industry team, led by Dr. Ron O'Malley of Nucor Steel, Decatur, Alabama, which are helping to conduct the plant measurements needed for model calibration, and are overseeing the implementation of the UIUC control algorithms into the level-2 control system of their plant. In addition, H. Castillejos is leading experimental efforts to better understand heat transfer in the spray zones. This project enhances and complements the modeling efforts at the University of Illinois Continuous Casting Consortium, created in 1989 by Prof. Thomas and currently supported by nine member companies.

Along with fundamental scientific benefits, the research proposed will have broader impacts. The direct broad impact of the effort proposed is quality improvement, cost reduction, and energy saving in continuous casting of thin steel slabs. This impact is strongly amplified by the rapid growth of thin slab casting in the steel industry. In addition, improved understanding of the control issues and algorithms will broadly benefit other high-speed manufacturing processes as well. The research will educate students who will take the modeling and control tools and technologies developed into industry. Most of all, the significant improvement of this key manufacturing process will be of direct benefit to society at large.

**2. The Process:** A schematic of steel processing is depicted in **Fig. 1**, with a close-up of the region between two rolls in the spray zone given in **Fig. 2**.

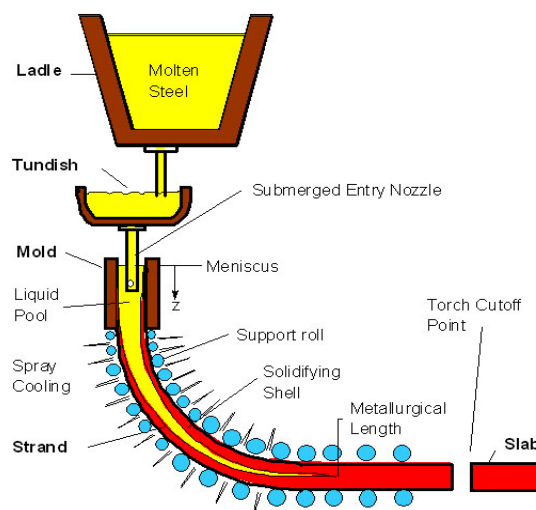


**Fig. 1.** Schematic of steel processing including ladle, tundish, and continuous casting

Steel flows from a ladle, through a “tundish,” and then exits down through a ceramic Submerged Entry Nozzle (SEN) into the mold. In the mold, the steel freezes against the water-cooled copper walls to form a thin solid shell, which is continuously withdrawn from the bottom of the mold at a “casting speed” that matches the flow rate of the incoming metal. The casting speed must be controlled to be slow enough to enable the shell to become sufficiently thick to support the liquid pool it contains, in order to avoid a catastrophic “breakout”, where molten steel penetrates the shell to drain over the bottom of the machine.

The steel strand then moves through the spray cooling zones, where water and air-mist sprays impact its surface to maintain cooling. Motor-driven drive rolls located below the mold continuously withdraw the strand downward. Many closely-spaced support rolls prevent the outward bulging of the shell due to the ferrostatic pressure arising from the liquid steel core. Water sprays emerge from high-pressure nozzles, which are interspaced between the support rolls and cool the strand during the solidification process. Other strategically placed rolls bend the shell to follow a curved path and then straighten it flat prior to torch cut-off into individual slabs. Start-up of this process is a relatively rare occurrence, and is achieved by inserting a “dummy” bar to plug the mold bottom.

The rolls support the the wide surface to prevent bulging, but greatly affect the temperature distribution. As shown in **Fig. 2**, sharp drops in surface temperature are experienced beneath each roll, and beneath the impacting spray jet. Reheating occurs in the adjacent regions which are protected thermally by the space under the rolls. Gravity significantly affects the water boundary layer, which causes cooling to vary above and below the jet, and between the inside and outside surfaces of the strand. The water spray rates should be continuously adjusted to maintain a desired surface temperature profile to avoid the formation of surface cracks. Cracks are caused by thermal stress combined with metallurgical embrittlement due to nonmetallic precipitates and grain growth, which depend mainly on cooling history. Spray control is difficult, because sensors such as optical pyrometers are often unreliable due to intermittent steam and surface emissivity variations. Thus, they cannot be used for online feedback-control.

After exiting the spray cooling zones, the steel strand surface reheats, as natural convection and radiation heat extraction is small. The strand is no longer supported by rolls, so should be fully solidified. If any liquid core remains beyond the zone of roll support, the strand will bulge catastrophically, creating a thick “whale” shape, that forces costly shutdown of the process.

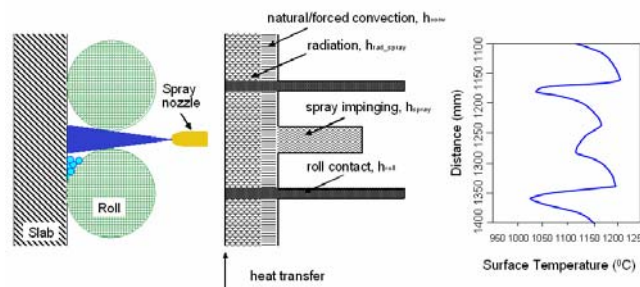


**Fig. 2** Schematic of the spray region of the thin-slab steel caster, and corresponding heat transfer, and surface temperature profiles.

**3. The Problem:** The strand is subject to a variety of cracking problems during secondary spray cooling, such as transverse midface and corner cracks. These surface defects require expensive surface-reconditioning or even rejection of the product. These quality problems are generally caused by non-optimal cooling conditions, which arise due to unaccommodated variations in the process, such as changes in casting speed or mold powder cooling conditions. Most operations simply scale the water flow rate with casting speed. This does not provide uniform cooling, however. For example, after a temporary drop in casting speed, the colder strand near the top of the caster will need less water for a long time, while the strand near the bottom of the caster will be gone in a short time. As another example, a change in mold powder crystallization can drop the heat flux temporarily, causing a region of hotter, thinner shell at mold exit, which requires more cooling for the rest of its time in the caster. The strategy for controlling the water flow rates in spray zones should dynamically adjust for each portion of the strand, according to its entire history.

Traditional control strategies to maintain the strand surface temperature to a desired profile would utilize feedback based on temperature measurement at various places in the spray zones. However, the intermittent surface scale layer and harsh environment of the steamy spray chamber makes optical temperature sensors unreliable. Thus, heuristic-based, open-loop control with a predictive model is the only successful control strategy to date. However, the model-based predictive control systems face special problems in thin slab casting, owing to the higher casting speed and the increased relative importance of solidification in the mold, which is not easy to predict accurately. Thin slab casters are more prone to cracking problems than conventional casters, which prevents them from entering certain markets. Thus, there is great incentive to develop an improved model-based control system to

optimize spray cooling, especially for the thin slab casting process.

**4. Current Results:** The results of this project are contained in 8 publications to date<sup>[2-9]</sup> and in our website <http://ccc.mechse.uiuc.edu>. This paper reports on seven different ongoing components of the current multifaceted research project:

- 1) Efficient fundamental model of solidification and temperature in thin slab casting: CON1D
- 2) Software Sensor, CONONLINE
- 3) Online control system development
- 4) Laboratory measurement of water flow and heat transfer during spray cooling
- 5) Steel plant experiments for model validation
- 6) Control of mold fluid flow
- 7) Understanding defect formation during continuous casting

**5. Efficient fundamental model of solidification and temperature in thin slab casting CON1D:** The finite-difference model, CON1D, is a simple but comprehensive fundamentally-based model of heat transfer and solidification of the continuous casting of steel slabs, including phenomena in both the mold and the spray regions.<sup>[10]</sup> The accuracy of this model in predicting heat transfer and solidification has been demonstrated through comparison with analytical solutions and plant measurements.<sup>[10]</sup>

The simulation domain of CON1D, shown in **Fig. 3**, is a transverse slice through the strand thickness that spans from the center of shell surface of the inner radius to that of the outer radius. The CON1D model computes the temperature and solidification history of the slice as it traverses the path from the meniscus down through the spray zones to the end of the caster.

CON1D solves the 1-D transient heat conduction equation within the solidifying steel shell:

$$\rho_{steel} C p_{steel}^* \frac{\partial T}{\partial t} = k_{steel} \frac{\partial^2 T}{\partial x^2} + \frac{\partial k_{steel}}{\partial T} \left( \frac{\partial T}{\partial x} \right)^2 \quad [1]$$

This fundamentally-based model predicts shell thickness, temperature distribution, heat flux profiles down the mold face, metallurgical length, and other phenomena. The calculation takes advantage of the high Peclet number of the process, which renders axial heat conduction negligible. Heat flux profile in the mold is based on the measured mold temperature rise and flow rate.

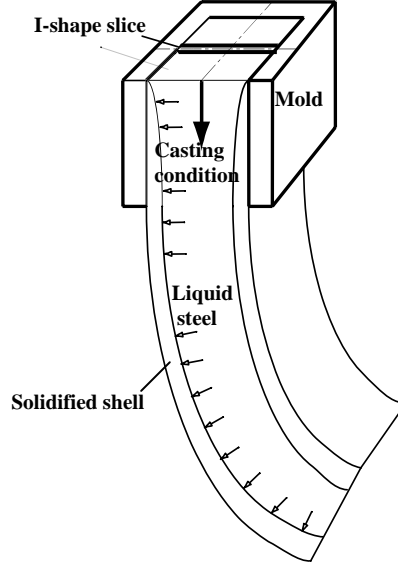


**Fig. 3.** CON1D simulation domain

Below the mold, heat flux from the strand surface varies greatly between each pair of support rolls according to spray nozzle cooling (based on water flux),  $h_{spray}$ ; radiation,  $h_{rad\_spray}$ ; natural convection,  $h_{conv}$ ; and heat conduction to the rolls,  $h_{roll}$ , as shown in **Fig. 2**. Incorporating these phenomena enables the model to simulate heat transfer during the entire continuous casting process. The heat extraction due to water sprays is a function of water flow<sup>[11]</sup> of the following form:

$$h_{spray} = A \cdot Q_{water}^c \cdot (1 - b \cdot T_{spray}) \quad [2]$$

where  $Q_{water}$  ( $l/m^2s$ ) is water flux in spray zones and  $T_{spray}$  is the temperature of the spray cooling water. The constants in this empirical correlation are modified from Nozaki<sup>[12]</sup>, which has been used successfully in previous models<sup>[11, 13]</sup>. Very recent experimental work is being undertaken as part of this project to measure these coefficients more accurately, including the effects of air mist cooling, and the enhanced heat transfer rates associated with intermittent boiling called the “Leidenfrost” effect.

Radiation is calculated by:

$$h_{rad\_spray} = \sigma \cdot \epsilon_{steel} (T_{sK} + T_{ambK}) (T_{sK}^2 + T_{sprayK}^2) \quad [3]$$

where  $T_{sK}$  and  $T_{sprayK}$  are  $T_s$  and  $T_{spray}$  expressed in Kelvin. Natural convection is treated as a constant input for every spray zone. For water-cooling only, it is not very important, therefore it is simplified to  $8.7W/m^2K$  everywhere. Larger values can be entered for  $h_{conv}$  to reflect the stronger convection when there is air mist in the cooling zone. Heat extraction into the rolls is calculated based on the fraction of heat extraction to the rolls,  $f_{roll}$ , which is calibrated for each spray zone. A typical  $f_{roll}$  value of 0.05 produces local temperature

drops beneath the rolls of about 100°C. Beyond the spray zones, heat transfer simplifies to radiation and natural convection. Further details on the model equations, boundary conditions, numerical discretization, previous validation efforts and other applications are given elsewhere.<sup>[10]</sup>

An example of the predicted surface temperature history of the slice is given in **Fig. 4**. Notice that there are a number of temperature peaks and dips. The temperature dips are caused by water spray impingement and roll contact, whereas the temperature peaks occur where convection and radiation are the only mechanisms of heat extraction.

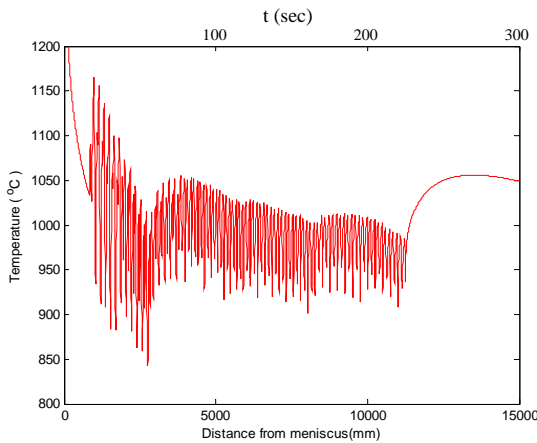


**Fig. 4.** Example of CON1D output: slice surface temperature history

The CON1D program has been optimized to run in less than 0.5s on a personal computer. This is necessary for it to become part of an online control system that updates every 1s.

In addition to successful model-based prediction and control capability, the model was used to generate setpoints for typical casting conditions. Specifically, 72 set points were generated for the Nucor caster to allow operation at 8 different spray-water patterns over a range of casting speeds (discretized as 9 different speeds over the maximum speed range). These set points are temperature profiles generated by CON1D using typical mold heat flux dependent on casting parameters which includes casting speed.<sup>[14, 15]</sup>

The model is now ready to calibrate, validate, and implement as a software sensor into a control system.

**6. Software Sensor CONONLINE:** Traditional feedback control of the secondary cooling sprays has not been implemented in commercial casters, primarily

due to the difficulty of operating sensors in the spray region. Optical pyrometers can be inaccurate due to emissivity variations from intermittent surface scale on the steel and diffraction through the water spray and steam. In this project, CON1D has been adapted to serve as a “software sensor” in place of hardware temperature sensors in a control system.

The purpose of the software sensor is to provide a real-time estimate of the temperature of the entire outer surface of steel strand. This is the same function temperature sensors would perform in a traditional feedback control system. This shell surface temperature history is denoted  $T(z, t)$ , where  $z$  is the distance from the meniscus and  $t$  is the time.

The output domain of CON1D on a  $t$ - $z$  plot is shown in **Fig. 5**. For constant casting speed, this domain is a line with slope  $\tan(\theta)$ . As the figure illustrates, at time  $t_0$ , CON1D only gives data for point  $z_0$ . In order to obtain the full temperature profile at time  $t_0$ , the results of multiple CON1D runs must be interpolated.

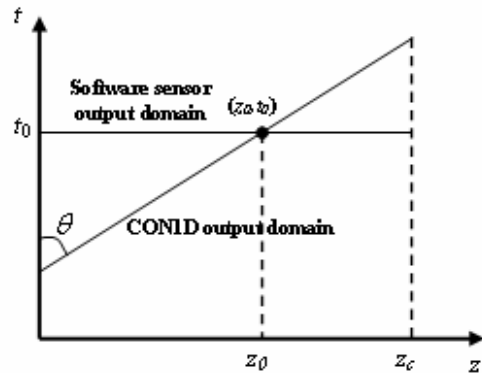


**Fig. 5.** CON1D and sensor output domain comparison

Keeping track of many slices through the moving shell requires increases computational time by a factor equal to the number of slices. However, it is not necessary to perform a complete run of every slice at each time step. Instead, each slice is simulated incrementally for the duration of each time step, which requires the same time as one complete simulation through the caster, ~0.6s. This is possible because conductive heat transfer is negligible in the casting direction, as discussed in the previous section. The shell surface temperature is then approximated by interpolating the latest temperature history of each slice. This process is illustrated in Fig. 6.

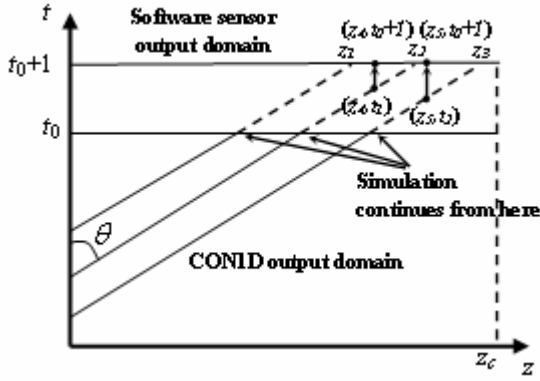


**Fig. 6.** Illustration of the incremental run of CON1D and shell surface temperature profile approximation

At time  $t_0$ , each of the slices is simulated for 1 second, until time  $t_0 + 1$ . For a caster of length 15 m operating at a casting speed of 3 m/min (50 mm/s), then  $15000 / 50 = 300$  slices are needed to continuously simulate the entire caster. In practice, 200 slices are used regardless of casting speed, in order to maintain a real time simulation.

At startup, CONONLINE creates new slices equally spaced throughout the caster. With 200 slices, in a 15 m long caster, there should be 75 mm between slices. Once the  $i^{\text{th}}$  slice is 75 mm from the meniscus, CONONLINE starts the  $i+1^{\text{th}}$  slice. During operation, a new slice is started every time an old slice reaches the end of the caster, keeping the total number of slices constant.

**Fig. 6** shows three consecutive slices. The slices are all started at different times, giving shell temperatures for different curves in the  $t$ - $z$  domain. Then at time  $t_0 + 1$ , exact data is known for points  $z_1$ ,  $z_2$ , and  $z_3$ . For  $z_1 < z < z_2$  and  $z_2 < z < z_3$ , an interpolation scheme must be used. As shown in **Fig. 7**, a linear interpolation scheme between the exact data points would miss a great deal of the data in the peaks and valleys, with temperature errors possibly of 100 or more. Instead, a delay interpolation scheme is used.

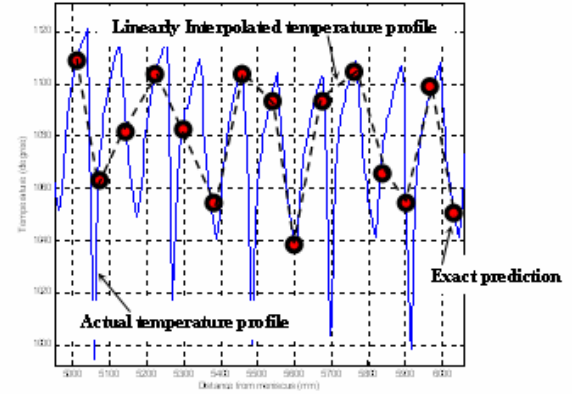


**Fig. 7.** Example of the actual temperature profile, the exact estimation/prediction and linearly interpolated temperature profile

This is done by using the history of the CON1D slice.  $T(z_4, t_0 + 1)$  in Fig. 6 is approximated by  $T(z_4, t_2)$  from the temperature history of the middle slice. Similarly,  $T(z_5, t_0 + 1)$  is approximated by  $T(z_5, t_3)$  from the temperature history of the right slice. In general,

$$T(z, t) = T_{1D}^i(z) \text{ if } z_{i+1}(t) < z \leq z_i(t)$$

where  $T_{1D}^i$  is the CON1D temperature history of the  $i^{\text{th}}$  slice and  $z_i(t)$ ,  $z_{i+1}(t)$  are the locations of the  $i^{\text{th}}$  and  $i+1^{\text{th}}$  slices at time  $t$ .

The approximation error under this interpolation scheme depends on the slice spacing. The average error can be estimated as the temperature change in half the time needed for a slice to travel the distance of slice-spacing. For 75 mm-spaced slices moving at 50 mm/s, this would be 0.75 s. The temperature change in this time is typically around 30 C, and goes to zero as the system goes to steady state. The present scheme is better than linear interpolation, which still has error at steady state.

The software sensor, CONONLINE, manages the multiple slices and their respective temperature histories, and interpolates between them. It uses CON1D as a subroutine to compute each slice. CONONLINE provides an estimate of the full shell surface temperature profile to use in control calculation. More detail is given elsewhere.<sup>[7]</sup>



**7. Online Control System Development:** A control system has been developed that integrates with the Level 2 system of a continuous caster, to control the spray water cooling flow rates in real time. The software implementation of this system includes 1) the software sensor CONONLINE, 2) a monitor to display the results in real time, and 3) a control algorithm CONCONTROLLER to regulate the surface temperature, in addition to network software to maintain communications and shared memory.

CONCONTROLLER currently runs on a separate computer from CONONLINE, to ensure real-time output of spray commands even if the model runs slowly or crashes. The monitor runs on the model workstation, and takes advantage of GTK+ and GDK graphical user interface libraries. The two computers communicate with each other and the caster Level 2 system as shown in

Fig. 8.

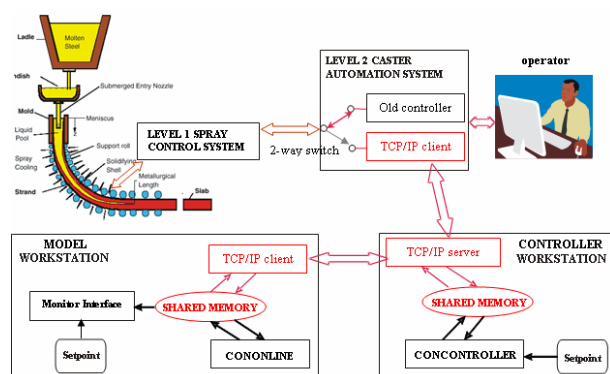


Fig. 8. Software sensor based control system architecture

Fig. 9 shows a typical snapshot of the monitor. It was developed to provide clear and quick feedback to the plant operators and engineers. The data shown includes shell surface temperature, temperature setpoint, shell profile, metallurgical length, spray water flow commands, and casting conditions. This allows for monitoring of the control system performance, warning of dangerous operating conditions, and providing general information about the current state of the steel slab.

The accuracy of control is limited first by the actual casting equipment. A continuous caster is divided into spray zones, each zone having a single water flow input. This water flow rate is the actuator controlled by CONCONTROLLER. Although there is usually more than one spray zone across the width of the caster, the output of the software sensor is only for the centerline

of the slab. The spray zones outside of the center of the caster require additional logic. Currently, they are fixed fractions of the central zone, simulated by the model.

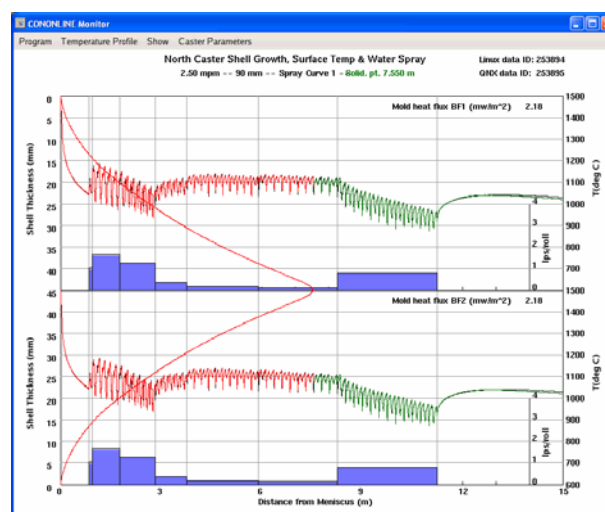


Fig. 9. Monitor interface displaying on both sides: the shell surface temperature profile, its corresponding setpoints, the spray-water flow rates commanded and their setpoints, the shell thickness profile prediction, and other information.

Fig. 10 shows the center spray zones of the caster at the Nucor Decatur steel mill. In the first four spray zones, inner and outer radius sprays are linked. In the remaining three zones, the inner and outer radius sprays may be separately assigned. Thus, a total of 10 independent spray commands are available.

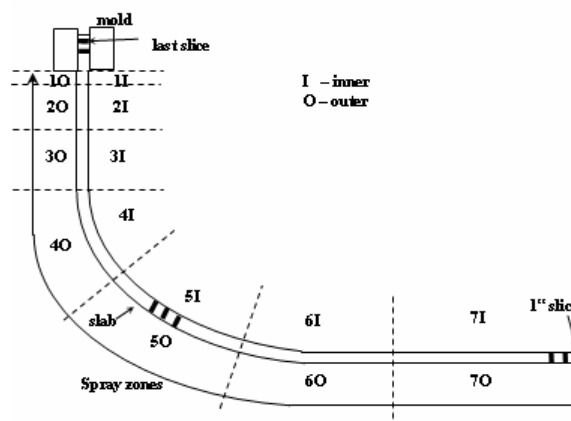


Fig. 10. Center spray area configuration

Surface temperature response from conduction is faster than heat transported by the moving strand along the length of the caster, so the control of each spray zone may be governed by an independent control algorithm. Currently, these are single-input-single-output

controllers. The possibility of using multiple-input-single-output or distributed-input controllers is a topic of continuing research.

Each controller follows the same general control algorithm. At each time step, the error between the shell surface temperature profile estimated by the software sensor and a setpoint temperature profile is averaged over the portion of the slab governed by the controller. This average temperature error is used to calculate control effort based on a proportional-integral control law. The gains are tuned separately for each spray command.

The actual spray command is limited to a range between turning closing the control valves and opening them completely, and so the effect of actuator saturation is a concern. Integrator windup can lead to over or undershooting should saturation occur during transient behavior. A classical anti-windup scheme<sup>[16]</sup> is applied to prevent integrator windup if the control command becomes negative or greater than the maximum possible spray rate. More detail on the controller design is given elsewhere.<sup>[7]</sup>

Choosing temperature setpoints is a challenging task that is on-going. Initial setpoints have been based on sets of water flow-rate setpoints that yield good performance in the steady state from past experience. A complete set of spray rates for all spray zones at all casting speeds is called a spray pattern. Each spray pattern is typically tuned for a specific grade of steel. It is designed to achieve a surface temperature history that avoids cracks, while solidifying the steel prior to exit from the containment region.

**Fig. 11** and **Fig. 13** show results of offline testing using the control system. These figures show the outputs of the software sensor under different control strategies in order to illustrate some of the issues involved in implementing software sensor-based control. Running in real time, they include the same numerical errors encountered in the caster. In partnership with Nucor Steel Decatur, the model is being tested on an actual caster in “shadow mode”, prior to implementing the control system commercially.

**Fig. 11** compares the performance of the online control system to the current spray practices during a rise in casting speed from 2 to 2.5 m/min. The shell surface temperature at 11.2 m below the meniscus, the end of containment in the simulated caster, is plotted. The conventional control scheme is based on interpolation between fixed water-flow setpoints.

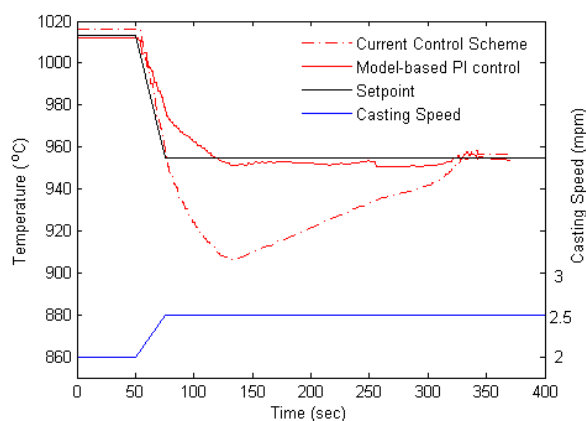


**Fig. 11.** Surface temperature histories predicted at 11200mm below meniscus for conventional and new model-based control systems, showing that new controller better tracks surface temperature during a change in casting speed

During transient operation, the water flow setpoints from a spray pattern are linearly interpolated by casting speed to determine the water flow rates used. Without regard to the actual dynamics of the casting process, the current conventional control scheme increases the water flow rates proportionally to the casting speed during casting speed rises, causing overcooling of the casting slab. In **Fig. 11**, the temperature undershoot caused by this issue can be seen. These problems associated with a conventional control scheme are addressed by the model-based PI control algorithm in CONCONTROLLER, which exploits the shell temperature profile estimated by CONONLINE (and CON1D). In this case, the controller attempts to match the temperature setpoint profiles that correspond to the steady-state water flow rate setpoints.

With the software sensor based control, it is also possible to use constant temperature setpoints. This can be thought of as changing the control objective to a disturbance rejection problem, maintaining the shell surface temperature at a given profile during transient changes in casting conditions. Instead of a different temperature profile for each casting speed, a single temperature profile is chosen for the setpoints. This retains the experience and knowledge in the current spray practices, while taking advantage of the opportunities added by the software sensor.

Another problem arises, regarding heat transfer in the mold. When calculating a temperature setpoint using CON1D, an estimated mold heat removal rate and pour temperature are used. If the actual running conditions differ, the setpoint temperature at mold exit may be



higher or lower than the actual temperature at mold exit. PI control, in this case, would try to eliminate this “error,” causing sharp transients in the spray zones just below the mold. However, the resulting fluctuations are more likely to cause cracking problems than the higher or lower temperature itself. To avoid these detrimental fluctuations, five different mold heat removal rates are used to create five different shell temperature setpoints. This is shown in **Fig. 12**.

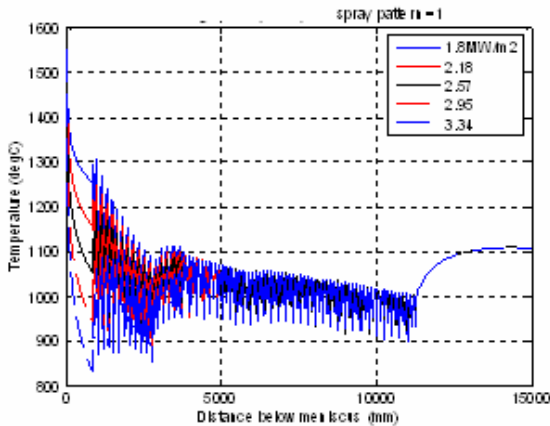
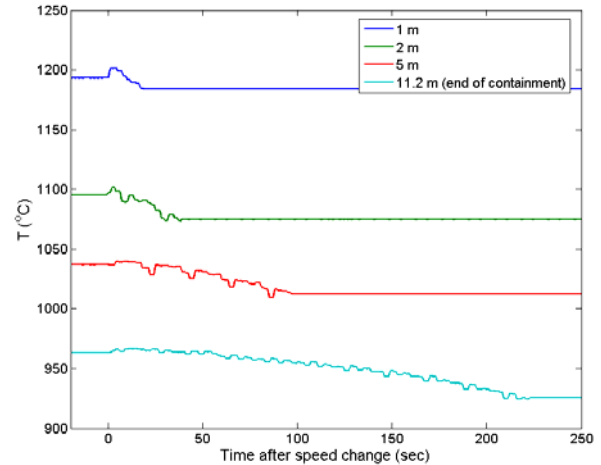


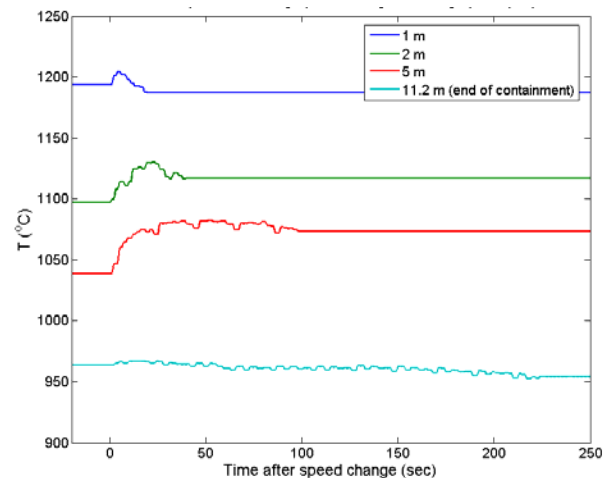
**Fig. 12.** The 5 temperature setpoint curves for spray pattern 1

Note that the effect of mold heat removal variations diminishes down the strand. The setpoint only needs to be adjusted in the spray zones higher up in the caster. Currently, the setpoint in the first four segments is interpolated linearly by the mold exit temperature. In the last three segments, the nominal setpoint is used.

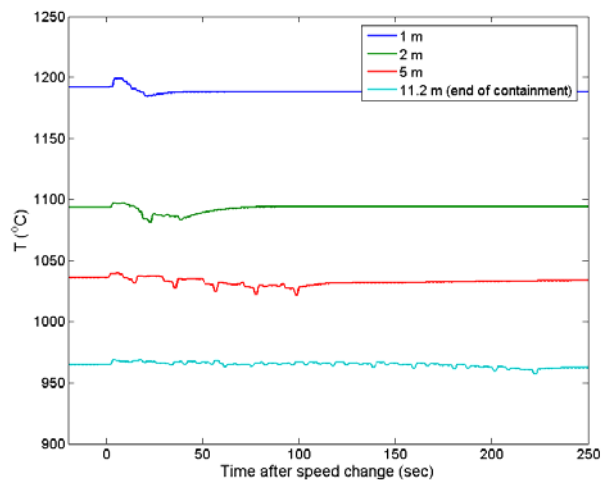
The following results show the software sensor outputs for three different control methodologies. In all cases, the casting speed drops suddenly from 3.5 m/min to 3.0 m/min at time  $t=0$ . In Fig. 13-A, no control is used, and so the water spray rates remain constant. Due to the lower casting speed, the resulting surface temperatures are lower. In Fig. 13-B, the current spray practice is followed. When the casting speed changes, the spray rates are immediately changed according to the predetermined spray pattern. In Fig. 13-C, the current CONONLINE-CONCONTROLLER online control system is used to set the water spray rates.



**A) No spray control (constant flow rates).**



**B) Conventional control (flow rates proportional to casting speed).**



**C) Software-sensor based PI control (constant temperature setpoints)**

**Fig. 13.** Outer shell surface temperature at different distances from meniscus after casting speed drop.

A few effects are observed in all three cases. There is a rise in temperature immediately after the casting speed changes due to the decrease in mold heat removal rate that accompanies the speed drop. This increase, as described above, decreases in magnitude lower down the caster. A small amount of periodic error can be seen in all three graphs. This is due to the delay interpolation described in section 6. Finally, steady state is not reached until the steel at every point in the caster has been cast entirely at the new conditions. The transient period therefore increases with longer distances from the meniscus.

If no control is used, the surface temperature drops throughout the caster due to the lower casting speed as shown in Fig. 13-A. Transient behavior with overshoots is produced by conventional control (Fig. 13-B). Note that the steady state change in temperature differs throughout the caster. At some distances, the final temperature is lower after the speed change while at others it is higher. This system does not account for the dynamics of the moving steel strand. The new software-sensor based control system avoids these problems, as the spray rates are changed sequentially to roughly achieve the desired steady state performance (Fig. 13-C).

This new software-sensor based control system will improve steel quality at the steel plant, by maintaining temperature in the process more closely during transients. An advantage of CONONLINE, beyond its use for control, is that it offers more information to plant engineers and operators regarding the effect that casting conditions have on the strand. Moreover, the system, which runs in real time and accurately represents the behavior of a real caster, is a valuable research tool that enables scientific investigation of the continuous casting process. Future advances in control strategies and quality understanding can now be investigated using this system.

**8. Laboratory measurement of water flow and heat transfer during spray cooling:** Experiments have been initiated as part of this project to gain a more fundamental understanding of water spray cooling at high temperatures.<sup>[8]</sup> The research focuses on the conditions found at the surface of the steel strand in the secondary spray cooling zones of steel continuous casting machine with water jet / air mist or “pneumatic” cooling. These conditions include a steel surface temperature range of 1300-700°C. Historically, hydraulic nozzles that only use water for cooling are used. Lately, pneumatic nozzles which force water out of the nozzle with pressurized air are becoming more

popular because cooling severity is less. These “air-mist” nozzles depend on the characteristics of spray, e.g. droplet size and velocity, and, as literature search before starting this research showed, not enough of fundamental knowledge is available to fully understand the cooling mechanism. This understanding is very important to developing and implementing better boundary conditions for heat transfer models in continuous casting and would allow better design of secondary cooling systems.

This research investigates the effects of different air and water pressures, water impact density, time scales of the transient phenomena at the hot surface, water composition, and surface roughness. The research is being conducted in Saltillo, Mexico in co-operation with Cinvestav, a national research organization, owing to availability of specialized laboratory facilities for this type of research, and previous successful research in this field being conducted by Drs. Castillejos and Acosta.<sup>[17]</sup>

The boundary condition for secondary cooling in CONONLINE is presented in Eq. 2. The coefficients of this model depend on careful measurement. It depends on the water condition at the interface, which involves film boiling and the Leidenfrost effect. When two layers form: water above a thin layer of steam, then the heat transfer is relatively steady. However, spray heat transfer is often dynamic and is a complex function of droplet momentum, surface roughness, and surface temperature. Pneumatic nozzles may increase the Leidenfrost temperature to such a high value that heat transfer is always in the transient boiling regime. Thus, further research is needed not just on measuring the heat flux during spray cooling, but also on understanding the nozzle characteristics which control this behavior. The collaboration with Cinvestav aims to investigate these issues, using both transient and steady-state experiments.

The apparatus shown in **Fig. 14**, is for transient cooling conditions, where a sample steel plate is heated to a desired temperature and then quenched using different values of air and water pressures.

The first step to understand how heat transfer occurs is to measure the impact density, i.e. amount of water impacting in a unit area in unit time. The spray water exiting the nozzle is measured for a specific time using an unheated plate perforated with holes connected to tubes, called a “water collector”. Impact density is calculated knowing the size of each collector hole and the spraying time. This is repeated for maximum and minimum operating conditions to see the changes caused by changes in water and air pressures. In **Fig. 15**,

typical results are shown for a nozzle at both maximum and minimum operating conditions.

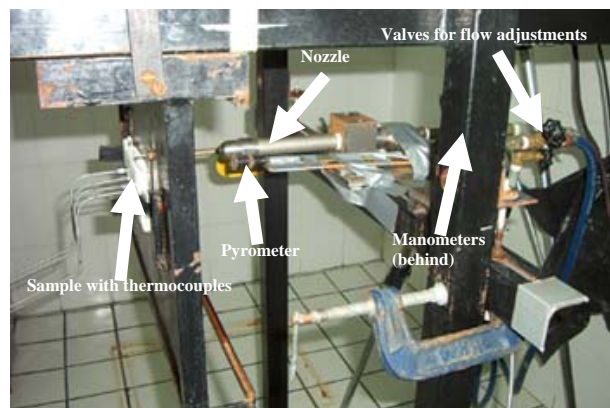


Fig. 14. Unsteady state measurement apparatus.

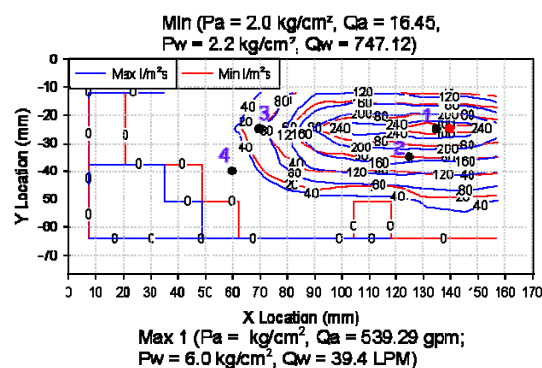


Fig. 15. Spray pattern corresponding to minimum and maximum operating conditions. Black dots thermocouple locations and the red dot is the nozzle centerline.

In this project, the spray patterns of all the Delavan Spray Technology nozzles used in the Nucor Decatur and Riverdale casters were measured. The water spray rate maps give the shape of the water droplet impact distribution over the height of the pattern and are needed for developing a fundamental-based model of heat transfer convection rates. This measurement also provides a simple method to maintain uniform heat transfer by showing how to position nozzles to cover the whole area it is designed to cool. During this research, it was found that two of the nozzles were not, in fact, covering the whole width of the area that they were supposed to cool as shown in Fig. 16.

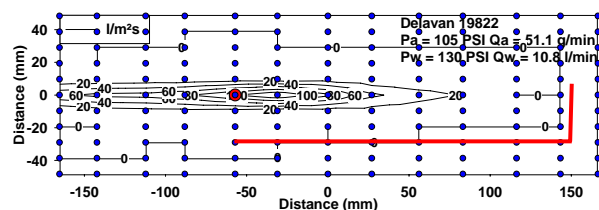


Fig. 16. Measured spray pattern and corresponding width from the caster blueprints marked a red line. Blue dots collector locations and the red dot is the nozzle centerline.

After the plate is instrumented with thermocouples at appropriate locations (based on the water collector results), it is heated up to between 700 and 1300°C, transported quickly to the spray station, and quenched down to room temperature. Typical measured cooling curves are shown in Fig. 17.

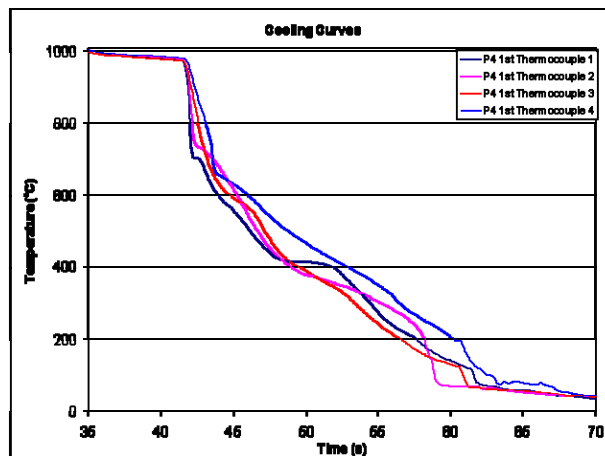
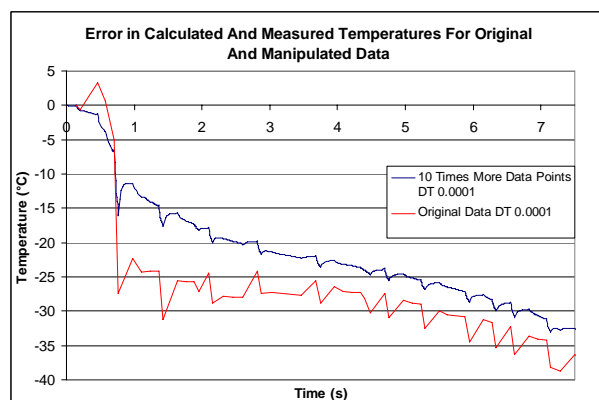


Fig. 17. Cooling curves from a transient experiment

Heat flux and temperature on the surface of a sample is determined using a computer program CONTA developed in Michigan State University and Sandia National Laboratories. The program solves nonlinear, one-dimensional planar inverse heat conduction problem (IHCP) using finite difference method (FDM) based on implicit Crank-Nicolson method. When measuring large cooling rates, the calculated heat flux has errors, as they do not reproduce the measured temperatures when used as the boundary condition of a direct heat transfer solver. To overcome this problem, the original data was augmented by linear interpolating new data between the measured data points. The correlation obtained can be seen from Fig. 18.



**Fig. 18.** Heat flux values from centre of a water spray nozzle impact pattern as a function calculated surface temperature.

Another approach to investigate spray cooling is to maintain the sample at a constant temperature while spraying it. An apparatus was designed and constructed for this purpose. A picture of the new apparatus is given in **Fig. 19**.

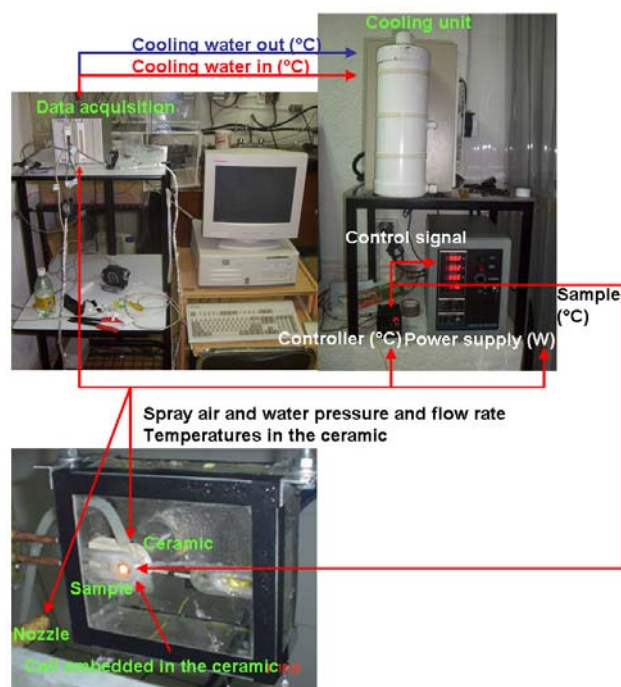


**Fig. 19.** New steady-state measurement apparatus.

The sample is sprayed and a thermocouple is used to monitor its temperature. This information is sent to a controller that maintains the temperature in the sample by controlling induction heating. Both the temperature of the sample and the power needed for maintaining the

temperature are recorded. From the recorded power it is possible to calculate the energy needed to maintain the temperature i.e. the energy extracted by environment and spray. With this apparatus, it is possible to measure transient heat extraction during the changes that occur during spraying at a constant temperature (due to boundary layer development, etc.) independently from the changes occurring due to changing temperature conditions.

Results from steady state measurements together with results from transient measurements are shown in **Fig. 20**.

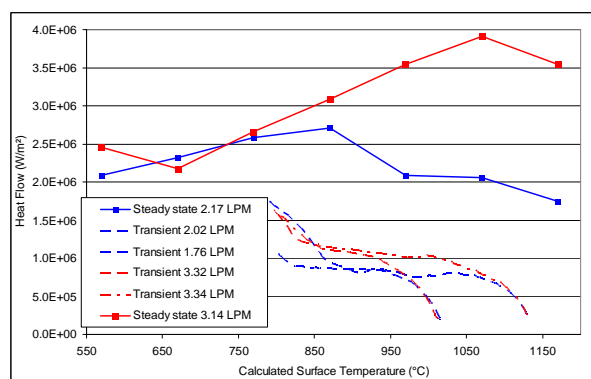


**Fig. 20.** Heat flux values from centre of a water spray nozzle impact pattern as a function calculated surface temperature.

It is difficult to draw firm conclusions from this experiment, owing to the difficulties in avoiding sample oxidation, measuring thermal efficiencies, extracting accurate temperatures and obtaining repeatable results. However, these preliminary results show that these measurements can be made and the preliminary results in **Fig. 20** suggest that the transient experiment produces much lower heat transfer coefficients than the steady state experiment. This might be due to the time needed to establish the boundary layers, or due to thermocouple delays. The initial portion of each transient experiment is similar. After several seconds, the transient measurements start to approach the steady-state predictions, as indicated by the similarity between the heat fluxes at 700°C and lower.

Future improvements, change material from steel to platinum, cooling water temperature measurements, new DAQ-system, and better insulation of the sample from moisture on other surfaces except the front, are planned to improve the ability to measure heat extraction. Also calculation of the surface temperature will be improved by using a 3D heat transfer model. More details on this work are given elsewhere.<sup>[8]</sup>

**9. Steel Plant Experiments for Model Validation and Calibration:** Experimental trials have been carried out at Nucor Steel, Decatur, Alabama, and at Mittal Steel, Riverdale, in order to measure slab surface temperature variations with optical pyrometers. In addition, mold heat flux is measured from the temperature rise of the cooling water, knowing the water flow rate. These results are being used to calibrate the CON1D model. Results for Nucor were presented previously.<sup>[5]</sup>

At Mittal Riverdale, surface temperature is measured for different casting speed and spray water flow rates using four pyrometers: including one at the bend, (10256mm below the meniscus), one at the shear, (14550mm below meniscus), and two in the spray zones. So far, three trials (trial 1 on Sep.11<sup>th</sup>, trial 2 on Oct.19<sup>th</sup> and trial 3 on Mar.12<sup>th</sup>) have been conducted at steady conditions. Simulations of six cases (case 1~6, two for each trial) have been performed to predict the strand surface temperature, which are then compared with the pyrometer measurements.

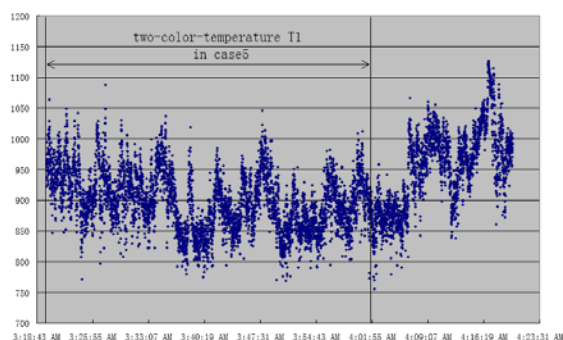


**Fig. 21.** Two-color-temperature T1 in case 5

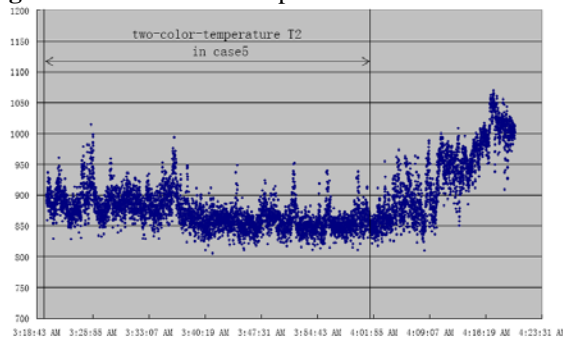


**Fig. 22.** Two-color-temperature T2 in case 5

The pyrometer measurements fluctuated throughout the trials, due to the intermittent presence of steam, possible variations in emissivity of the surface scale layer, and changes in casting conditions. Time periods of steady casting, with relatively uniform pyrometer temperatures, were chosen to get average measured temperatures.

**Fig. 21 and Fig. 22** show typical spray-zone pyrometer measurements for case 5 in trial 3. These pyrometers were put in the same location of segment 2, 5361mm below meniscus. Pyrometer measurements varied by 20°C between different two-color methods and 200°C over 90 minutes time intervals of roughly steady casting. The ~40-minute time period over which the measured temperature is averaged, is also shown in the figures.

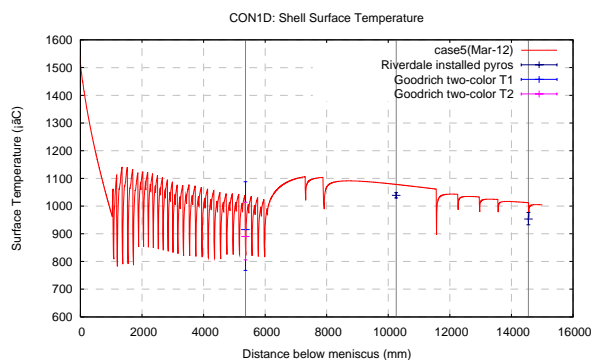


**Fig. 23.** Temperature prediction and comparison

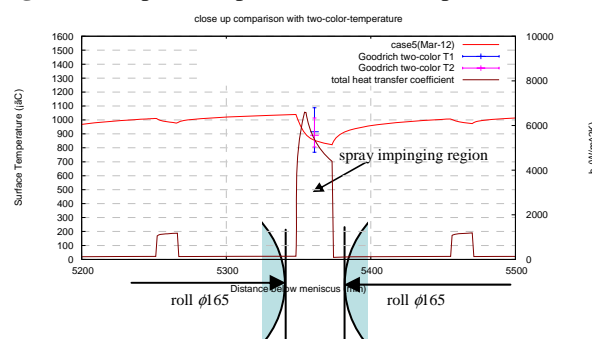


**Fig. 24.** Close up comparison with two-color-temperature

**Fig. 23 and Fig. 24** show simulation results for case 5. Measurements from the pyrometers are included for comparison. The model temperature predictions are mainly within the scatter of the measurements, so are considered to be reasonable. This degree of agreement was also found for most casting conditions in other cases, especially within the spray zones.

The results from this run show that the entire processing time for this 55-mm thick strand from liquid to complete solidification takes only 1-2 minutes. A casting speed of 4.5m/min results in a metallurgical length of 4.6m for this typical thin slab caster.

Validation and improvement of the CON1D model is still ongoing. In the meantime, the model has been implemented into the CONONLINE control model system and is being tested in the plant, where quantitative accuracy is not essential to improve over the existing control model.



**10. Understanding Defect formation during Continuous Casting:** To gain maximum benefit from a new spray-water control system, it is important to have a fundamental understanding of how defects form in the process. Parallel research is ongoing to achieve this aim. Work has been initiated to gain new insight into the mechanism of formation of defects associated with secondary spray cooling. These surface defects often initiate in the mold<sup>[18]</sup>, especially at the meniscus<sup>[19]</sup>, and later form surface cracks far below the mold in the secondary spray cooling zones. Cracks form at the roots of oscillation marks, which are prone to transverse crack formation during the spray cooling, depending on the temperature history. Thus, oscillation mark depth is also being studied. To avoid cracks, it is often necessary to keep the strand above a certain critical temperature, such as the  $Ar_3$  temperature,  $\sim 700^\circ C$ .

**11. Control of Mold Fluid Flow:** Many casting defects are caused by problems with fluid flow in the mold. To control fluid flow in the mold, an electromagnetic brake (EMBr) force is applied in many thin slab casters, including Nucor. A computational fluid flow model has been developed and applied to investigate the effects of varying SEN submergence depth and EMBr field strength on flow in the mold cavity<sup>[9]</sup>. The three-dimensional, steady  $k-\epsilon$  model of the nozzle and liquid cavity in the mold used the magnetic induction method in FLUENT to incorporate the localized-type static EMBr field measured at a steel plant. The model was validated by comparing results with an analytical solution and with nail board and oscillation mark measurements collected at the plant (see Fig. 25). Increasing EMBr strength at a constant SEN depth is found to cause a deeper jet impingement, weaker upper recirculation zone and meniscus velocity, and a smaller meniscus wave. Increasing SEN depth without EMBr caused the same trends. Increasing SEN depth at a constant EMBr strength brought about the opposite: higher meniscus velocity, larger meniscus wave, and deeper penetration depth. Using the knowledge gained from this model, electromagnetic forces can be controlled to stabilize the fluid flow in the mold cavity and thereby minimize casting defects.

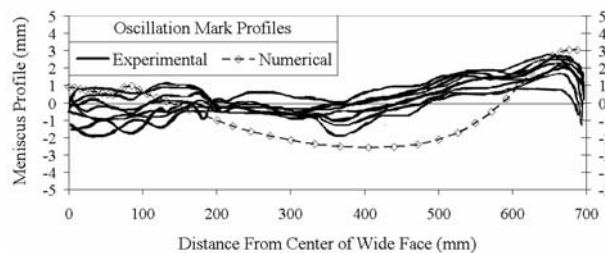


**Fig. 25.** Comparison of calculated meniscus profile from Case 6 with oscillation marks

**12. Advanced Control Algorithm Development:** Rejection of broad classes of disturbances in systems with unknown parameters, but known parameter structure is a nontrivial practically important problem. In the finite-dimensional case, this problem is typically addressed through adaptive control laws modified to reject the disturbance class of interest. However, the standard finite-dimensional adaptive control configurations, such as those falling under MRAC, do not, in general, transition into the infinite-dimensional setting in a well-posed manner. Therefore, attaining similar disturbance rejection performance in distributed parameter case presents a considerable challenge.

This setting is of interest in a solidifying shell temperature control in continuous steel casting, where a single two-dimensional boundary control problem of the outer shell surface temperature shown in Fig. 1 can be well approximated by a pair of one-dimensional distributed control problems of the outer shell surface temperature for the inner and the outer caster radii. This is accomplished by bringing in, as shown in the Fig. 26 below, the near-constant distributed disturbance.

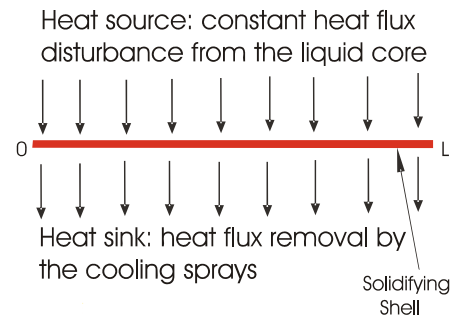


**Fig. 26.** Approximation of the single 2D shell surface temperature boundary control problem by the two - outer and inner radii - 1D shell surface temperature distributed control problems through the introduction of the constant distributed heat flux disturbance. The latter is induced at the liquid/solid interface by the molten steel core encased by the solidifying shell

The latter is characterized by an approximately known model and represents the heat flux at the interface between the inner surface of the solidifying shell and the liquid core. The disturbance is seen to lie in the system input space. Thinking along the lines of this approximation governs, to a large extent, current spray cooling control practice at some key steel casting facilities.

In this application, actuation is designed to be a very close approximation of the distributed one to ensure smooth cooling along the strand - the feature especially

important in continuous thin slab metal casting due to the thinness of the solidifying shell, and a matching pyrometer array temperature sensing is being currently developed. The parameters of the casting process, such as heat transfer coefficients, are known to be periodic-like functions of a spatial variable due to the fact that the outer shell surface alternates between being in contact with the fixed position support rollers and being subject to the water flux from the sprays along the cooling zone of a caster. This functional dependence is known, however, only approximately, is influenced by a number of factors, such as steel grade and casting speed, and undergoes a slow time-variation caused by the solidifying shell motion. Reduction of uncertainty in this dependence is currently underway; however it proves to be very costly, time consuming, and requiring nontrivial instrumentation. In addition, the pyrometer readings are characterized by a noticeable steam-induced spatiotemporal noise. \

This problem is solved in [4]. Based on the well-posed MRAC configurations recently introduced [2] that are free from plant output spatial derivatives, this work develops the well-posed error systems and the corresponding robust MRAC laws with disturbance rejection for a class of systems represented by parabolic or hyperbolic PDEs with spatially varying parameters. Disturbances are assumed to be generated by a known model and lie in the system input space. Control signal is, then, shown to include the disturbance estimate generated by the corresponding distributed parameter Luenberger-type observer. The well-posed error systems and the corresponding algorithms for parabolic and hyperbolic PDEs are derived, with the disturbance rejection properties exhibited in numerical simulations. For simplicity, derivations are carried out for a single spatial domain. The paper considers distributed sensing and actuation as well as distributed disturbance.

Plant:  $u_t = (a(x)u_x)_x + b(x)u + f(x, t) + d(x, t)$

Reference Model:  $v_t = (a_1(x)v_x)_x + b_1(x)v + r(x, t)$

Adaptive control law:  $f = r + \varepsilon_0 e + \eta_{d1} v_{xx} + \eta_{d2} v_x + \eta_b v$

Disturbance model:  $d_t = (a_d(x)d_x)_x + f_d$

Schematics of adaptive controller and disturbance observer is given by **Fig. 27**.

**12. Conclusions:** This report has summarized the results of seven different sub-projects which comprise this multi-faceted research project. Further details can be found in 8 publications [2-9] and in the website <http://ccc.mechse.uiuc.edu>.

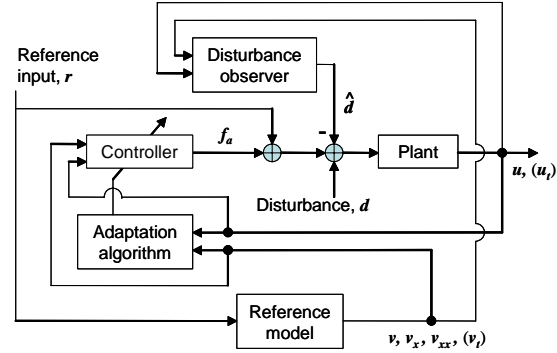


**Fig. 27.** Adaptive controller and disturbance observer

**13. Acknowledgments:** This work is supported by the National Science Foundation (Grant # DMI-0500453) and the Continuous Casting Consortium at the University of Illinois. Thanks are also extended to industry collaborators at Nucor Steel, Decatur, AL, including Ron O'Malley; Delevan Spray Technologies, including Stephen Swoope and Mittal Riverdale, including Clint Graham. The authors also wish to thank the National Center for Supercomputing Applications at the University of Illinois for computing time.

#### 14. References:

1. "World Steel in Figures," International Iron Steel Institute, Brussels, Belgium, [www.worldsteel.org](http://www.worldsteel.org), 2004.
2. Kim, J. and J. Bentsman, "Robust Adaptive Control of Parabolic and Hyperbolic Systems with Spatially-varying Parameters," 44th IEEE Conference on Decision and Control, (Seville, Spain, Dec. 13-15, 2005), 2005, 1503-1508.
3. Kim, J. and J. Bentsman, "Multiresolution Finite-Dimensionalization of Parameter Update Laws in Adaptive Control of Distributed Parameter Systems," 45th IEEE Conference on Decision and Control, (San Diego, CA, Dec. 13-15, 2006), 2006, 2801-2806.
4. Kim, J. and J. Bentsman, "Disturbance Rejection in Robust Model Reference Adaptive Control of Parabolic and Hyperbolic Systems," 45th IEEE Conference on Decision and Control, (San Diego, CA, Dec. 13-15, 2006), 2006, 3083-3088.
5. B.G. Thomas, J. Bentsman, K. Zheng, S. Vapalahti, B. Petrus, A. Behera, A.H. Castillejos and F.A. Acosta, "Online Dynamic Control of Cooling in Continuous Casting of Thin Steel Slabs," in Proceedings of 2006 NSF Design.

- Service, and Manufacturing Grantees and Research Conference, W. DeVries and M. Leu, eds., (St. Louis, Missouri, July 24-27, 2006), 2006, 11p.
6. Kim, J. and J. Bentsman, "Disturbance Rejection in Robust Model Reference Adaptive Control of a Class of Distributed Parameter Systems," International Journal of Adaptive Control and Signal Processing (submitted), 2007.
  7. Zheng, K., B. Petrus, B.G. Thomas and J. Bentsman, "Design and Implementation of a Real-time Spray Cooling Control System for Continuous Casting of Thin Steel Slabs,," in AISTech 2007, Steelmaking Conference Proceedings, Indianapolis, May 7-10, 2007, Association for Iron and Steel Technology, Warrendale, PA, USA, 2007.
  8. Vapalahti, S., B. G. Thomas, S. Louhenkilpi, A.H. Castillejos, F. A. Acosta and C.A. Hernandez, "Heat Transfer Modelling of Continuous Casting: Numerical Considerations, Laboratory Measurements and Plant Validation," STEELSIM 2007, (Graz, Austria, Sept. 12-14, 2007), 2007.
  9. Cukierski, K. and B.G. Thomas, "Flow Control with Local Electromagnetic Braking in Continuous Casting of Steel Slabs," Metals and Materials Transactions B (in press), 2007.
  10. Meng, Y. and B.G. Thomas, "Heat Transfer and Solidification Model of Continuous Slab Casting: CON1D," Metal. & Material Trans., Vol. 34B (5), 2003, 685-705.
  11. Brimacombe, J.K., P.K. Agarwal, S. Hibbins, B. Prabhaker and L.A. Baptista, "Spray Cooling in the Continuous Casting of Steel," Vol. 2, Continuous Casting, ISS/AIME, Warrendale, PA, 1984, 109-123.
  12. Nozaki, T., "A Secondary Cooling Pattern for Preventing Surface Cracks of Continuous Casting Slab," Trans. ISIJ, Vol. 18, 1978, 330-338.
  13. Hardin, R.A., H. Shen and C. Beckermann, "Heat Transfer Modeling of Continuous Steel Slab Caster Using Realistic Spray Patterns," Modelling of Casting, Welding and Advanced Solidification Processes IX, (Aachen, Germany, 20-25 Aug. 2000), TMS, Warrendale, PA, 2000, 729-736, 190.
  14. Thomas, B.G. and C. Ojeda, "Ideal Taper Prediction for Slab Casting," ISSTech Steelmaking Conference, (Indianapolis, IN, USA, April 27-30, 2003), Vol. 86, 2003, 396-308.
  15. Cicutti, C., MartinValdez, T. Perez, G. DiGresia, W. Balante and J. Petroni. Mould Thermal Evaluation in a Slab Continuous Casting Machine. Steelmaking Conference Proceedings. Vol. 85 (2002), 97-107.
  16. C. Edwards and I. Postlethwaite, "Anti-windup and Bumpless Transfer Schemes," UKACC International Conference on CONTROL, 1996, 394-399.
  17. Castillejos A. H. et. al, in Proc. of 33rd McMasters Symp. on Iron & Steel Making, 2005, 47-58.
  18. Meng, Y. and B.G. Thomas, "Simulation of Microstructure and Behavior of Interfacial Mold Slag Layers in Continuous Casting of Steel," ISIJ International, Vol. 46 (5), 2006, 660-669.
  19. Sengupta, J., B.G. Thomas, H.J. Shin, G.G. Lee and S.H. Kim, "Mechanism of Hook Formation during Continuous Casting of Ultra-low Carbon Steel Slabs," Metallurgical and Materials Transactions A, Vol. 37A (5), 2006, 1597-1611.